ISSN 1075-7015, Geology of Ore Deposits, 2008, Vol. 50, No. 8, pp. 815–826. © Pleiades Publishing, Ltd., 2008.
Original Russian Text © N.V. Chukanov, V.A. Dubovitsky, S.A. Vozchikova, S.M. Orlova, 2008, published in Zapiski Rossiiskogo Mineralogicheskogo Obshchestva, 2008, Pt CXXXVII, No. 1, pp. 77–93.

METHODS OF RESEARCH OF MINERALS, ROCKS, AND ORES

Discrete and Functional–Geometric Methods of Infrared Spectroscopy of Minerals Using Reference Samples

N. V. Chukanov, V. A. Dubovitsky, S. A. Vozchikova, and S. M. Orlova

Institute of Problems of Chemical Physics, Russian Academy of Sciences, Chernogolovka, Moscow oblast, 142432 Russia

Received August 10, 2006

Abstract—Different methods of infrared spectroscopy applied to the analysis of mineral phases using spectra of reference samples are compared. Traditionally (discretely), the IR spectrum is processed as pairs of numbers characterizing frequencies and intensities of separate bands. The major advantage of such an approach is the opportunity to visualize fine crystallochemical features within groups of related minerals. An alternative technique is based on functional–geometric analysis, dealing with the spectral curve as a whole. This approach is based on the minimization of root-mean square deviations and opens up wide possibilities for the identification of minerals by their IR spectra. The crux of the functional–geometric method is the determination of a linear combination of standard spectra with nonnegative coefficients that ensures the best (in terms of integral functional comparison) approximation of the analyzed spectral curve. As a rule, the spectra of minerals with the closest crystallochemical relationships with the examined sample make the greatest contribution to this resolution. Numerous examples of application of the discrete and functional–geometric methods are described.

DOI: 10.1134/S1075701508080205

INTRODUCTION

Despite a number of advantages of infrared (IR) spectroscopy as a rapid and very informative method for identification of minerals, its mineralogical application is restricted, partly due to tradition, but mainly because of the absence of sufficiently complete datasets and effective algorithms and programs allowing automated identification. Note that the overwhelming majority of applications of IR spectroscopy are based on the idea of an unequivocal relationship between the absorption curve and the substance. Thus, the problem consists of measuring a spectrum as accurately as possible and carrying out its identification.

The traditional way of IR analysis is determination of the positions and intensities of a small encoding set of separate narrow characteristic spectral bands and their comparison with an available atlas of experimental standard spectra. This permits the determination of mineral species and estimation of the content of chemical groups. However, in this case, the information from unresolved bands, the amount of which considerably exceeds observed absorption maximums, is lost.

In recent decades, techniques of standard-free IR spectroscopy based on quantum-chemical calculations, setting and solving of inverse problems, and group-theoretical analysis of the symmetry of crystal structures have been developed (*Vibrational*…, 1977; *Modern*…, 1990). However, these approaches are currently only of academic interest because of a low accuracy of quantum-chemical calculations, inadequate mathematical models of the formation of recorded IR spectra related to innumerable local situations, and laborious calculations.

Another approach (also traditional) for obtaining information on local symmetry in the crystal structure of a mineral is based on group-theoretical analysis. However, the practical application of this method meets fundamental and often insurmountable obstacles. The correct computation of the active bands attributed to normal vibrations of this type is possible only after resolution of a spectrum into individual Voigt components, which is in itself a rather incorrect mathematical problem because of ambiguous results of such resolution within the limits of allowable errors. However, even knowing the number of individual components, as a rule, it is difficult to separate the splittings related to symmetry factors and resonance. In the case of solid solutions (isomorphic series), this problem becomes practically unsolvable due to a great number of local situations.

Over a long time, we collected and analyzed reference samples and recorded their IR spectra with application of frequency standards. To date, the working collection of reference spectra includes 3000 spectral records, embracing 2000 mineral species. Due to a substantial increase in the amount (almost by an order in comparison with available analogues) and a significant improvement in the quality of spectrograms, as well as in comparison sample reliability, certain progress has been achieved in the application of IR spectroscopy to the study of minerals on the basis of comparative analysis of the spectrum of an examined mineral and reference spectra. In particular, a number of new mineral species differing from known analogues in symmetry,

Corresponding author: N.V. Chukanov. E-mail: chukanov@icp.ac.ru

cation ordering, topology of the structural framework, and other features that are with difficulty identified by X-ray patterns and chemical composition but clearly expressed in characteristic splittings and shifts of IR bands have been discovered. Some examples of such analysis based on application of characteristic bands are described in the first section of this paper.

At the next stage of investigation, we proceeded to the development of ways to extract information from IR spectra operating with the spectral curve as a whole. On the one hand, knowledge of the absorption curve in a wide range of frequencies makes it possible to effectively solve the problem of identification of matter having broad lines on the basis of reference spectra. For this purpose, it is sufficient to introduce an integral functional (for instance, quadratic) that quantifies the level of comparison of spectrum deviations. Thus, the introduction of a comparative functional significantly expands the possibilities of classic analysis because a substance is encoded by the entire spectral curve rather than by a set of bands. On the other hand, a possibility arises for implementing integrated standard analysis, which does not require a spectrum of the sought substance in the database. The procedure of such analysis is based on additivity of optical densities and consists of the best approximation of an analyzed spectrum by linear combination of reference spectral curves. This method is based on the assumption that, in the case of a good approximation, the proportions of components obtained will allow a conclusion to be drawn about the microstructure of the analyzed substance. Nominally, the method consists of solving an inverse problem to determine the nonnegative vector of "composition" that ensures the best fitting of an experimental spectral curve in sense of an integral comparison functional, with ranging of weights of reference basis spectra and a scattering curve with variable parameters. The result is presented as coefficients of spectral resolution by the basis of reference spectra of specific substances or (with a corresponding grouping) by classes of substances. The geometric sense of such an approximation is projecting an examined spectrum on a convex cone of spectra of possible component mixtures in the linearly normalized space of all spectral curves. This extremal problem is closely related to the method of optimal integral approximation of the search for a nonnegative solution of a first-order integral equation (Dubovitsky and Milyutina, 1985; Dubovitsky and Irzhak, 2005) and inherits the high stability characteristic of this method. A mathematical formulation and examples of application of this promising approach are given in the second section of this paper.

THE DISCRETE METHOD OF INFRARED SPECTROSCOPY OF MINERALS

In the discrete representation, an IR spectrum is described as pairs of numbers characterizing the frequencies and intensities at the points corresponding to the absorption maximums (peaks) and points of inflection in spectral curves (shoulders). Tables of IR spectra in the discrete mode can be used to identify minerals like tables of X-ray powder patterns. In particular, the analogy of IR spectra with X-ray patterns is expressed in similarity of spectra of isostructural minerals, shift of bands as a result of isomorphic substitutions, and splitting of bands in the case of symmetry lowering. The reason for this analogy is clear: the X-ray powder pattern reflects the coordinates of atoms in the unit cell, number of electrons on these atoms, and space symmetry; the IR spectrum reflects similar characteristics, including the position of atoms, their weights, the strength of interatomic bonds, and the local symmetry. However, while X-ray diffraction techniques are especially sensitive to the crystallochemical features of some minerals, IR spectroscopy is such a method for other minerals. Let us consider a few characteristic examples.

Effect of symmetry. The crystal structure of the roscherite-group minerals (Chukanov et al., 2006) is based on a heteropolyhedral framework composed of atoms with tetrahedral and octahedral coordination. The general crystallochemical formula of monoclinic (space group $C2/c$) roscherite-group minerals (roscherite proper, greifensteinite, zanazziite, and ruifrancoite) may be written as $Ca_2D_2M_4Be_4(PO_4)_6(OH)_4X_2 \cdot 4H_2O$, where D and M are octahedral cations Mg, Mn^{2+}, Fe^{2+}, Zn, Fe^{3+}, and Al. Site D is substantially vacant, with the degree of occupation usually ranging from 1/3 to 1/2. X is OH or H_2O. The triclinic members of the roscherite group (Fanfani et al., 1977), including the recently described atencioite (Rastsvetaeva et al., 2004; Chukanov and Moeckel, 2005), are attributed to a second subgroup; the individuality of atencioite was proved for the first time by IR spectroscopy. The structures of these minerals are topologically similar to their monoclinic analogues. However, the lowered symmetry results in breakdown of D and M sites into pairs of nonequivalent sites, which can be occupied in different ways. Thus, the general formula of minerals of this subgroup may be expressed as $Ca_2D(1)D(2)M(1)_2M(2)_2Be_4(PO_4)_6(OH)_4X_2 \cdot 4H_2O$. In comparison with the monoclinic analogues, the amount of independent phosphorous sites in the triclinic species increases from 2 to 3; beryllium, from 1 to 2; OH groups (at the junction of M-octahedrons and Be-tetrahedrons), from 1 to 2; and H_2O molecules (incorporated into the Ca-polyhedron), from 1 to 2. This leads to additional splitting of the IR bands attributed to the vibrations of corresponding polyhedrons. Thus, atencioite (space group $P\bar{1}$) is characterized by additional (in comparison with monoclinic members of the roscherite group) splittings of bands of P–O stretching vibrations (doublet at 1031 + 1019 cm^{-1}), Be–O stretching vibrations (doublet at 721 + 709 cm^{-1}), and stretching vibra-

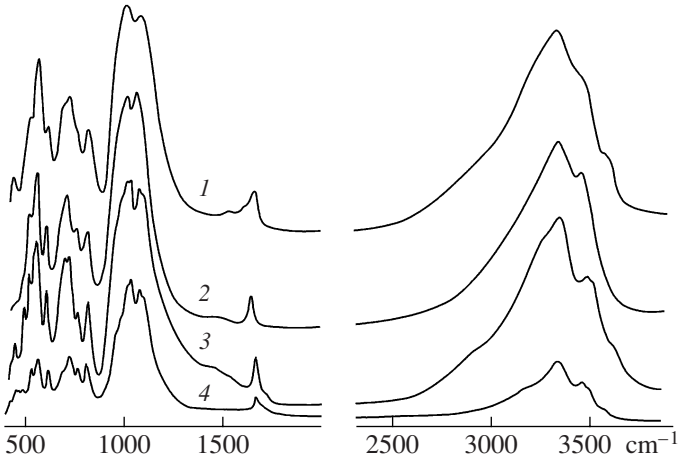

Fig. 1. Infrared spectra of the roscherite-group minerals: (*1*) ruifrancoite (monoclinic, Fe^{3+} dominant); (*2*) greifensteinite (monoclinic, Fe^{2+} dominant); (*3*) atencioite (triclinic analogue of greifensteinite); (*4*) triclinic, Mn dominant.

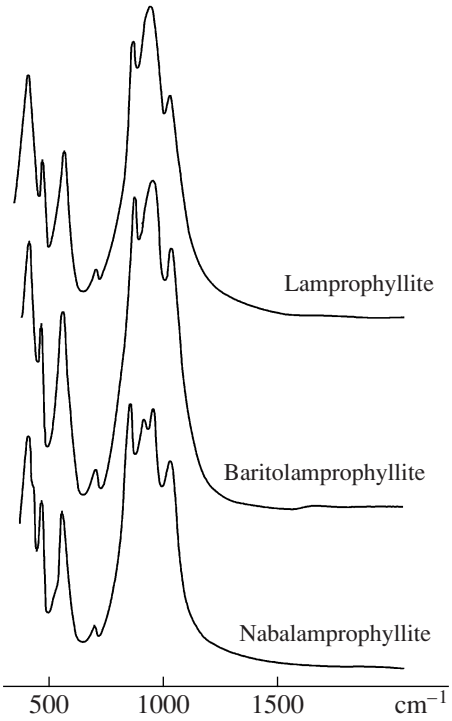

Fig. 2. Infrared spectra of the lamprophyllite-group minerals.

tions of octahedrons (absorption maximums at 522, 491, and 449 cm^{-1}) (Fig. 1).

Another example of the effect of symmetry on IR spectra is nabalamprophyllite $Ba(Na,Ba)[Na_3Ti(Ti_2O_2Si_4O_{14})(OH)_2]$, which clearly differs from all previously studied samples of lamprophyllite and baritolamprophyllite from the Khibiny, Lovozero, Murun, and Inagli plutons in a pronounced doublet at 954–921 cm^{-1} in the region of Si–O stretching vibrations involving apical O atoms, whereas, in the spectra of the lamprophyllite–baritolamprophyllite series, $(Sr,Ba,K)_2[Na_3Ti(Ti_2O_2Si_4O_{14})(OH)_2]$, only one band occasionally complicated by a weak shoulder is observed (Fig. 2). As commonly occurs, the splitting of the IR band in this case is a result of lowered symmetry of the crystal structure. In contrast to centrosymmetric (space group *C*2/*m*) lamprophyllite and baritolamprophyllite, where Si sorogroups are equivalent, the structure of nabalamprophyllite (space group *P*2/*m*) contains two types of Si_2O_7 groups. As a result, the single site of interstack cations characteristic of lamprophyllite and baritolamprophyllite is broken down into two unequivalent sites in nabalamprophyllite, one of which is occupied only by Ba and the other of which is dominated by Na. The two different sorogroups cause the aforementioned splitting of the band of Si–O stretching vibrations in the IR spectrum.

Eveslogite and yuksporite are titanosilicates extremely close in chemical composition and physical properties. Their crystal structure is not resolved by direct methods due to the absence of suitable single crystals. However, it is known that these minerals are characterized by different symmetry, which allows their identification by IR spectra. The lowering of symmetry from orthorhombic (for yuksporite) to monoclinic (for eveslogite) results in additional splittings of stretching vibrations of Si–O–Si bridges (arrows in Fig. 3). It may be suggested that the lowered symmetry in the case of eveslogite is related to different types of Si–O–Si bridges.

Isomorphic substitutions expressed in IR spectra. Cationic and anionic isomorphic substitutions are differently displayed in IR spectra. The mid-IR region is characterized by vibrations of fragments containing covalent bonds. The effect of substitutions in the cationic portion is indirectly demonstrated by a shift of bands attributed to complex anions (as rule, oxygen, AlF_6, and others). Isomorphic substitutions involving O-bearing anions may be observed in the IR spectrum directly from characteristic bands of these anions.

Many silicates, phosphates, and sulfates contain additional anions (CO_3, SO_4, BO_3, $B(OH)_4$, Cl, OH, etc.), polyatomic cations (NH_4, H_3O, UO_2, etc.), and neutral molecules (H_2O, CO_2). These particles are frequently composed of elements with low atomic numbers, and this hampers their identification with microprobe techniques. The members of the cancrinite, sodalite, scapolite, eudialyte, apatite, and ettringite groups; heterophyllosilicates, and kalborsite are examples of such minerals. Application of IR spectroscopy allowed the identification of a number of mineral species in the eudialyte group with CO_3^{2-} as the major additional anion (Fig. 4). In some alkaline ultramafic plutons, such minerals are typomorphic (Chukanov et al., 2005). The structural diversity of the eudialyte-group minerals is determined, to a great extent, by the

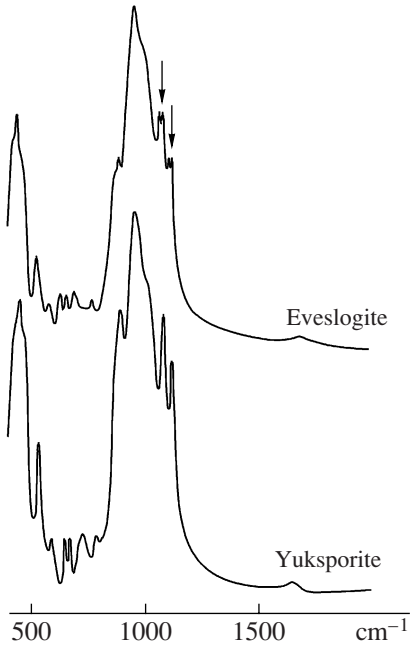

Fig. 3. Infrared spectra of eveslogite and yuksporite.

group of atoms linking neighboring Ca,O-octahedrons. The statistical analysis of IR spectra of eudialyte-group minerals, including the majority of samples with studied structures, made it possible to reveal the bands that are characteristic of these groups: NbO_4 (plane square) at 551–555 cm^{-1}, $Fe^{2+}O_4$ (plane square) at 540–544 cm^{-1}, TaO_4 (plane square) at 534 cm^{-1}, ZrO_4 (plane square) at 529–531 cm^{-1}, $(Mn,Fe)O_5$ (tetragonal pyramid) at 520–525 cm^{-1}, and FeO_6 (octahedron) at frequencies less than 500 cm^{-1} (Chukanov et al., 2003b).

IR spectroscopy applied to uranium minerals from the Bota-Burum deposit (Kazakhstan) resulted in the identification of arsenate uranium mica with ammonium as a major interlayer cation (recently, the mineral was approved by CNMMN IMA with the name uramarsite) (Fig. 5). Previously, this mineral was considered hydrogen uranospinite.

Shirokshinite, $K(NaMg_2)Si_4O_{10}F_2$ (Pekov et al., 2003), a new mineral of the mica group, in the structure of which Na occupies an octahedral site, is a typical example of the effect of cation isomorphic substitutions on the IR spectrum. The IR spectrum of shirokshinite is similar to its structural analogue taeniolite, $K(LiMg_2)Si_4O_{10}F_2$. However, the substitution of lithium by heavier sodium resulted in an additional shift of most bands (Fig. 6).

Effect of framework topology. The reliable identification of polymorphs and polytypes of minerals characterized by commensurable unit-cell dimensions usually requires the application of X-ray single crystal diffraction. However, in a number of cases, IR spectroscopy ensures identification of such minerals. In this respect, clinobarylite, $BaBe_2Si_2O_7$ (monoclinic, *Pm*, a = 11.618, b = 4.904, c = 4.655 Å, β = 89.94(2)°), as a dimorph of orthorhombic barylite ($P2_1na$ or *Pmna*, a = 11.65, $b \approx 9.8$, $c \approx 4.65$ Å) (Chu-

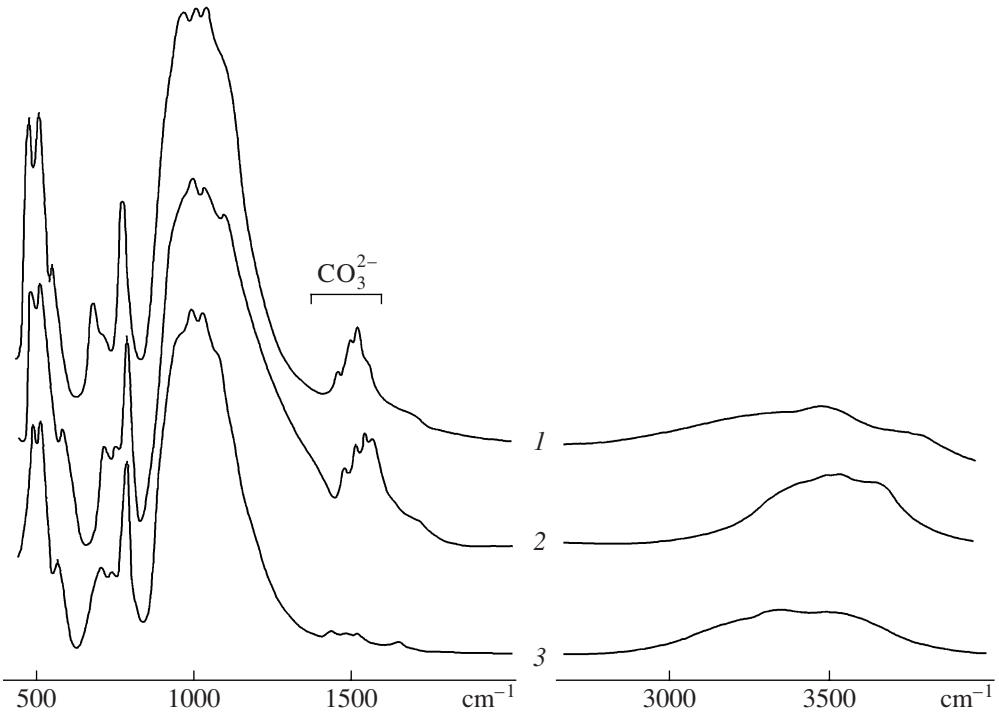

Fig. 4. Infrared spectra of (*1*) mogovidite, (*2*) golyshevite, and (*3*) feklichevite.

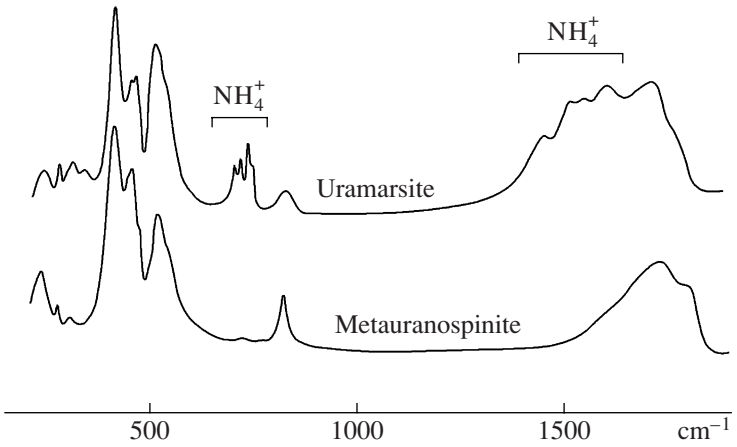

Fig. 5. Infrared spectra of uramarsite and metauranospinite.

kanov et al., 2003a), is an instructive example. According to X-ray patterns and most physical characteristics, both dimorphs are close to each other, but their IR spectra are strikingly different (Fig. 7).

Only a few examples of application of discrete IR spectroscopy to identification of minerals and discovery of new mineral species were considered above, but these examples are rather characteristic. The compilation of a sufficiently complete library of reference spectra made it possible to pass from use of IR spectroscopy for resolving particular problems to its wide application as a diagnostic method. Further progress is related to passage from discrete IR spectroscopy to approaches that use the information contained in the entire spectral curve.

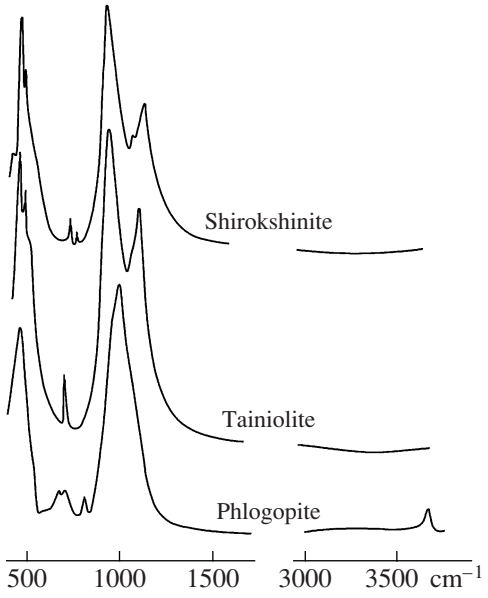

Fig. 6. Infrared spectra of trioctahedral magnesium micas.

FUNCTIONAL–GEOMETRIC METHOD OF INFRARED SPECTROSCOPY OF MINERALS

Analysis of a mixture of mineral phases on the basis of a linear model. In this section, we focus on determination of the quantitative composition of a mixture of substances on the basis of its IR spectrum and the spectra of expected components. This is the ground for the functional–geometric method discussed below. A more complete version including averaging of data

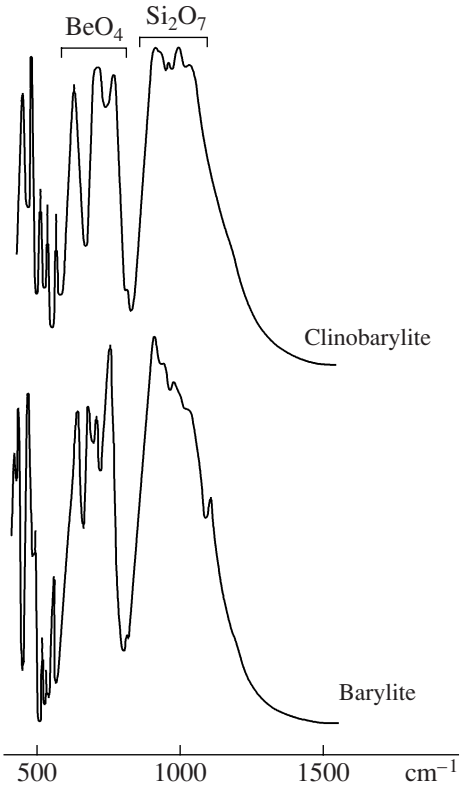

Fig. 7. Infrared spectra of clinobarylite and barylite.

was previously described by Dubovitsky et al. (2004). The mathematical model assumes a linear contribution of absorption coefficients to the spectrum of the mixture (the additivity principle). This assumption is fulfilled with a high accuracy in the medium-frequency IR region (10^{13}–10^{14} s^{-1}).

Let us consider a flat layer of homogeneous matter L (cm) thick, through which a plane-parallel flow of IR radiation passes. We designate the intensity of flow at a depth l at a frequency ω (rad/s) as $I(l, \omega)$ (J/cm^2). As follows from the additivity principle, $I(l, \omega)$ obeys the equation

$$\partial I(l, \omega)/\partial l = -k(\omega)I(l, \omega), \quad (1)$$

where $k(\omega)$ (cm^{-1}) is the absorption coefficient of matter in the layer as a function of frequency. The integration of (1) by l leads to the standard formula

$$k(\omega)L = \ln[I(0, \omega)/I(L, \omega)]. \quad (2)$$

Let us suggest now that the considered matter is a mixture of n components with volumetric fractions α_j and absorption coefficients $k_j(\omega)$. Then, according to the additivity principle, the relation $k(\omega) = \sum_j \alpha_j k_j(\omega)$, known as Beer's law, is true (Pohl, 1963). Therefore, formula (2) passes into expression

$$\sum_{j=1}^{n} \alpha_j k_j(\omega)L = \theta(L, \omega), \quad (3)$$

where $\theta(l, \omega) = \ln[I(0, \omega)/(l, \omega)]$ is a function of the absorption of IR radiation at a depth l at a frequency ω. On the basis of Eq. (3), the problem of determination of composition vector coefficients α_j can be set if is assumed that functions $k_j(\omega)$ of the components are known. Unfortunately, real measurements of the IR spectrum of mineral contain a number of uncertainties that are not taken into account in Eq. (3). First of all, this is related to difficulties in precise determination of the thickness of the layer L and to the effect of scattering and the uncertain amount of substance used as an immersion medium (commonly KBr). Let us write a more realistic mathematical model of the experiment. Assume that a fraction of substance β_j with number j, layer thickness L_j, absorption function θ_j, and scattering coefficient at unit length $k_j^p(\omega)$ (cm^{-1}) occurs in the experiment to determine $k_j(\omega)$. Designating a fraction of substance, scattering, and thickness in the experiment as β, $k^p(\omega)$, and L, respectively, and following the derivation of formulas (1) and (2), we obtain

$$\theta_j(L_j, \omega) = k_j(\omega)L_j\beta_j + k_j^p(\omega)L_j, \quad (4)$$

$$\theta(L, \omega) = \sum_j k_j(\omega)\alpha_j L\beta + k^p(\omega)L, \quad (5)$$

where, as above, α_j is the volumetric fraction of substance j. Expressing k_j in (5) through θ_j, we obtain

$$\sum_j x_j\theta_j(L_j, \omega) + \xi(\omega) = \theta(L, \omega), \quad (6)$$

where $x_j = (\alpha_j L\beta/(L_j\beta_j))$, $\xi(\omega) = k^p(\omega)L - \sum_j k_j^p(\omega)\alpha_j L\beta/\beta_\varphi$.

In practice, only approximated experimental values of absorption functions for some frequency range $\Omega = [\omega', \omega'']$ are known, and equality (6) is fulfilled inaccurately as well. Since combined equations (6) are approximated and overdetermined (a continuum of linear equations relative to x_j for frequencies from the range Ω), one can speak about recovery of the composition vector x only in a generalized sense, associating with expression (6) a problem of the best reproduction of the left part of equality (6) by the experimental absorption function $\theta(L, \omega)$. The generalized solution implies solution of the following minimization problem:

$$F(x, \xi) = \int_\Omega \left| \sum_{j \in J} x_j\theta_j(L_j, \omega) + \xi(\omega) - \theta(L, \omega) \right|^p d\omega \longrightarrow \min \quad (7)$$

at $x_j \geq 0$, $j \in J$, and $\xi \in \Xi$ relative to the vector $x \in R^n$ and the function ξ in the linear subspace Ξ of linear combinations of probable components of scattering (4) and (5). In this case, J is the subset of integer indexes within the range $l, \ldots, n$ and p is the number that satisfies the inequality $p \geq 1$, called the Hölder factor and determining the norm of function spaces, which estimates the mismatch of the right and left parts of Eq. (6). The parameter p controls the sensitivity of functional (7) to "overshoots" in experimental θ_j and θ (the sensitivity monotonically depends on p), whereas the set of indexes J determines the inventory of basis spectra used. In practice, a two-dimensional subspace of polynomials $\xi(\omega) = c_0 + c_1\omega^{-4}$ with sign-unfixed coefficients c_0 and c_1 is sufficient to describe the scattering. This corresponds to the description of scattering composed of components of pure reflection and coherent Rayleigh scattering (Pohl, 1963). A significant increase in dimension Ξ leads to an unwarranted decrease in the correctness of the model as a whole. A mathematically accurate pair solution (x^{min}, ξ^{min}) of convex programming problem (7) always exists. With easily made assumptions on functions θ_j and subspace Ξ, the assembly of all generalized solutions is resistant to distortions of experimental functions that are minor in the integral L_p norm.

In practice, there is a finite set of nodes ω_i ($i = l, \ldots, m_\Omega$) with known absorption functions θ_j and θ. Instead

of continuous extremal problem (7), we consider its discrete approximation

$$\sum_{i=1}^{m_\Omega} \nu_i \left| \sum_{j \in J} x_j \theta(L, \omega_i) + \xi(\omega_i) - \theta(L, \omega_i) \right|^p \longrightarrow \min \quad (8)$$

at $x_j \geq 0$, $j \in J$, and $\xi \in \Xi$, where ν_i is the set of positive weighting coefficients characterizing the significance of nodes ω_i. This is a finite-dimensional problem of minimization of a convex function on pair vectors (x, ξ) with the limitation of nonnegativity imposed on the x component. The ways of numerical solution of (8) are various and depend on the Hölder factor $p \geq 1$ included in the recovery scheme. Thus, at $p = 1$, expression (8) is converted into the equivalent problem of linear programming and solved by a finite algorithm of the simplex method. At $p > 1$, the minimization is effectively carried out by iteration of second-order descent combined with logarithmic penalty of the inequality constraints of nonnegativity (Fiacco and McCormick, 1968). The obtained solution x requires several Newton-type iterations before computer accuracy with respect to the value of the minimized function is attained. We implemented this algorithm in the form of a program in Fortran 95. In the important particular case at $p = 2$, Eq. (8) is a problem of the linear least squares method with a limitation of nonnegativity on part of the components; the finite NNLS algorithm (Lawson and Hanson, 1974) is known for its solution. Standard programs implementing the simplex method and NNLS algorithm are available from the Maple and MATLAB software packages. The computational capabilities of the algorithms listed and applied by us have an order $\min(m, |J|)^2 \max(m, |J|)$ of operations, where $|J|$ is the number of elements in the set of J indexes.

The condition of nonnegativity of x included in expressions (7) and (8) is extremely important because its removal results in a sharp decrease in information value and stability of recovery. Solution of problem (8) gives a nonnegative composition vector x, in which proportions of components x_i/x_j differ from the true ratio of volumetric fractions α_i/α_j by fixed multipliers $(L_i\beta_i)/(L_j\beta_j)$ dependent on the set of absorption basis functions θ_j, but independent of the absorption θ of the mixed substances.

Functional–geometric analysis of spectral curves. The geometric meaning of solution of extremal problem (7) is a projection of a function (the element θ) on a convex finite-faced cone $K[J] = \{\sum_{j \in J} x_j \theta_j(L, \omega) + \xi(\omega)$: $x_j \geq 0$, $j \in J$, $\xi \in \Xi\}$ generated by the forming bases and linear subspace of scattering. It is assumed that functions of frequency ω are considered in the normalized Hölder's space $L_p(\Omega)$. There are various approximations depending on the inventory of the index set of basis functions J included in Eq. (7).

In the minimum limiting case, there is one index; i.e., $J = \{j_0\}$. Then, problem (7) implies comparison of a studied spectrum θ with the basis spectrum θ_{j0} (with account and recovery of the unknown proportion of substance weight and distortion by scattering); the resultant discrepancy $F(x^{\min}, \xi^{\min})$ is the estimate of spectrum mismatch. The one-dimensional version of the algorithm's work is the most rapid and allows an exhaustive search for the closest reference sample among all candidates j_0 of the database by the criterion of the least mismatch. Thus, the one-dimensional version of algorithm (7) combined with enumeration of all available options is a direct generalization of standard IR analysis using reference samples. The obvious drawback of such analysis is that, in the successful case, it indicates with adequate accuracy an identical (or the closest to that examined) mineral from the database, for example, pertaining to the same mineral species, isomorphic series, or group, but, in the opposite case, only rejects the hypothesis of pertaining to the database without giving any information on the properties of the substance.

In the general (multivariate) case, we have an opportunity to estimate the arrangement of the element θ and the cone $K[J]$ of probable spectra of the substance mixture from a class of indexes J. If spectra of the database are divided into nonoverlapping classes—sets of indexes $J_1, \ldots, J_N$, then it is reasonable to estimate the belonging of an unknown substance to one of these classes by the least deviation of the spectrum θ from the cone $K[J_s]$. Such a version of the algorithm's work is a natural generalization of IR analysis of a mixture over classes of reference substances. For example, if the least discrepancy takes place for the spectrum cone of sorosilicates, whereas analysis in particular bases corresponding to other classes (for instance, phosphates or arsenates) or other silicate subclasses (nesosilicates or phyllosilicates) gives much worse fitting, this implies that the examined mineral pertains to sorosilicates.

Finally, taking a maximum set of indexes $J^{\max} = \{1, \ldots, n\}$, we analyze the arrangement of the spectrum θ and the cone $K[J^{\max}]$. The resolution of the projection of θ on the cone bears information on the crystallochemical cognation of the examined substance with a known one. Examples of this maximum version of the work of projective algorithm (8) are given below. Note that although the projection of θ on the cone is unambiguously determined, generally speaking, its resolution by the forming θ_j and the scattering space Ξ is ambiguous, probably due to the linear dependence of basis functions on θ_j. A unique resolution will be achieved by passing to marginal directions of the cone $K[J^{\max}]$. The elucidation of such a true basis is important because it is marginal directions that appear to be linked with independent centers absorbing IR radiation. However, these questions are subjects of future investigations beyond the scope of this paper.

Experimental and mathematical processing. In all cases considered below, the spectra of minerals enclosed in a pellet with excess KBr were recorded on

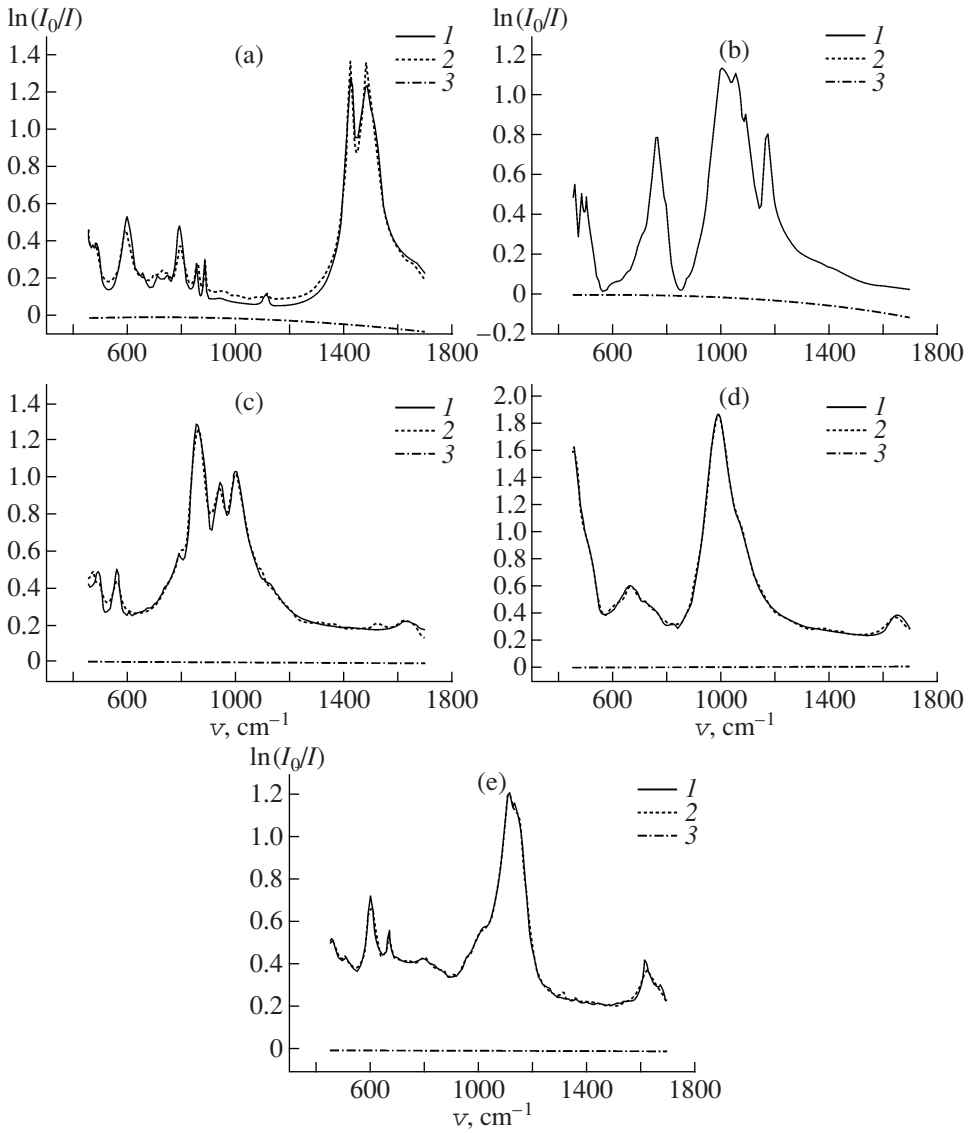

Fig. 8. Examples of good approximation. Results of functional–geometric analysis of IR spectra of (a) hydromagnesite, (b) telyushenkoite, (c) sodium boltwoodite, (d) vermiculite, and (e) gordaite. (*1*) Primary spectrum; (*2*) synthesized spectrum; (*3*) scattering correction line.

a Specord 75 IR dual-beam analog optical spectrophotometer within wavenumber ranges 400–1800 and 3000–3800 cm^{-1} and with a resolution of <3 and <8 cm^{-1}, respectively. A blank KBr disk was placed under the reference beam. Reference lines were inserted with wavenumber standards (polystyrene and gaseous ammonia). Further, each spectrogram was scanned with 150 dpi resolution and, after hand removal of defects (inscriptions, spots) from the BMP raster file, was digitized with a special program. This semiautomated approach made it possible to convert spectra of primary graphic form to digital form, used by the program of solution of (8), quite accurately and quickly (the number of discrete frequencies $m = 500$ for the basic diagnostic range 400–1800 cm^{-1}, and the relative error is less than the noise component of ~1%). Certainly, a more direct and improved mode of preparing data is use of a modern digital IR spectrometer. However, in creation of an IR spectrum database, spectrograms inevitably must be scanned from books and journals due to inaccessibility or, in a number of cases, absence of reference samples. A dataset including approximately 1400 digitized IR spectra of mineral species recorded in the ranges of medium frequencies is used in this study.

In the examples presented below, the composition vector was calculated according to scheme (8) at a Hölder factor $p = 2$. In Figs. 8 and 9, the wavenumber $\nu = \omega/(2\pi c)$, where c is the speed of light, is shown instead of the angular frequency ω, and the numbers 1, 2, and 3 indicate the initial spectrum, its projection on the

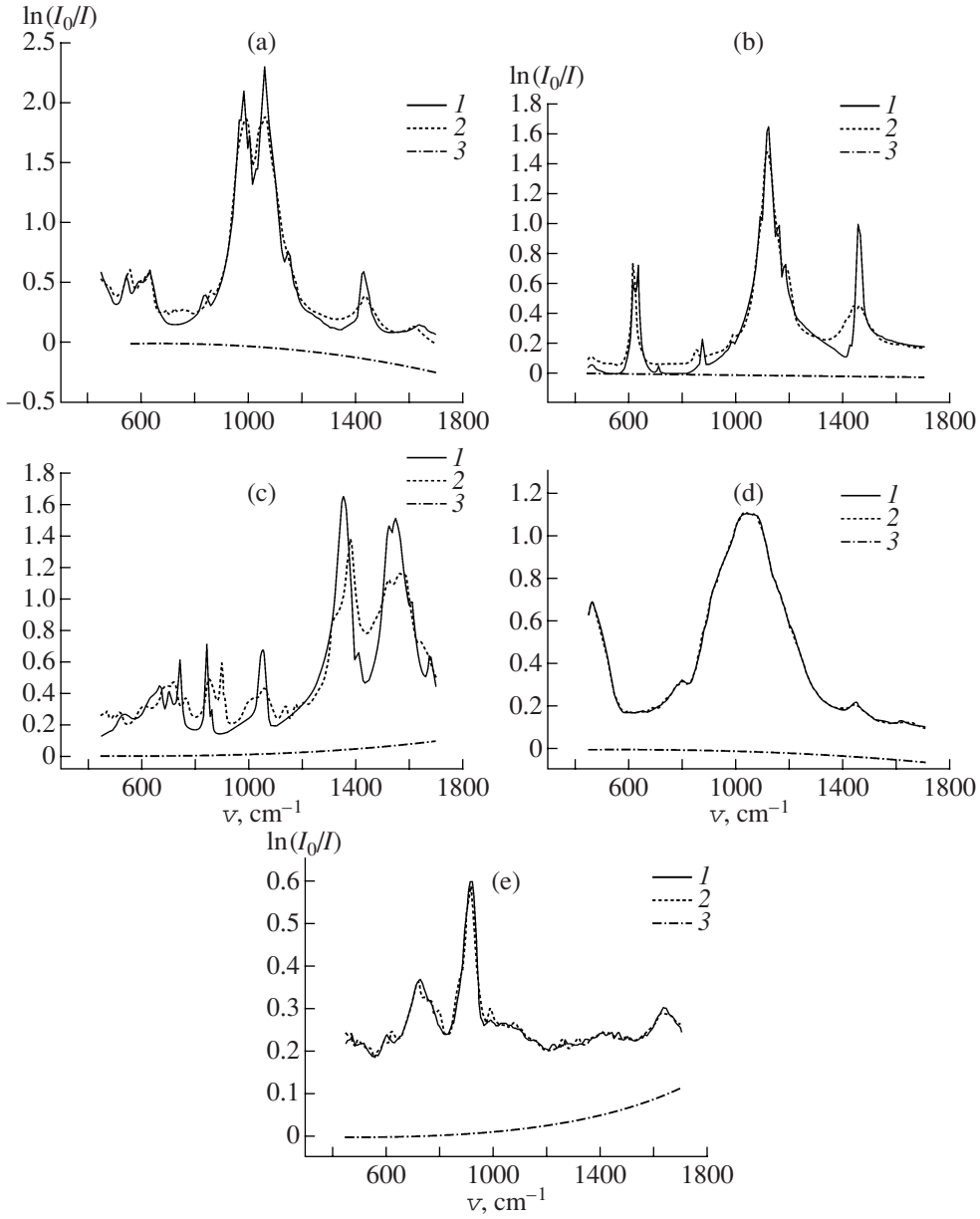

Fig. 9. Examples of poor approximation. Results of functional–geometric analysis of IR spectra of (a) spheniscidite, (b) hanksite, (c) weloganite, (d) ekanite, and (e) studtite.

cone of spectra of mixed components, and the curve of the calculated contribution of scattering, respectively.

The components of the database are grouped on the basis of their pertaining to a certain class of minerals according to their chemical composition (oxides, fluorides, carbonates, silicates, arsenates), and each class is divided into subclasses differing in the type and set of oxygen-bearing groups (for example, nesosilicates, sorosilicates, chain silicates, phyllosilicates, tectosilicates, and others are recognized in the class of silicates; heterosilicates, e.g., beryllosilicates and borosilicates, are separate subclasses; uranoarsenates are recognized in the arsenate class).

The method described above and the program developed on its basis were tested according to the aforementioned variant of projection on the maximum cone of the spectra of all substance mixtures. For this purpose, each reference spectrum was removed by turns from the basis and the resolution of the projection was analyzed on the rest of the basis. In most cases, such a procedure leads to the good approximation of a positive linear combination of a small number of basis spectra of minerals, mainly similar to the analyzed mineral in crystal chemistry (i.e., pertaining to the same class of chemical compounds and/or close in structure). In this way, the type of a substance that is not contained in the reference

database may be accurately determined. However, in a number of cases, the identification is unsatisfactory in some respect. Some typical examples are considered below.

Examples of successful analysis. When the examined mineral was presented in the basis by the spectrum of another sample of the same mineral, it was recognized automatically. An example of such recognition, hydromagnesite, $Mg_5(CO_3)_4(OH)_2 \cdot 4H_2O$, from the Bazhenovo chrysotile asbestos deposit in the Urals, is shown in Fig. 8a. The quality of fitting is satisfactory. The nonzero contributions to the resolution gave only ten spectra, i.e., only 1% of the basis; 89% of the contribution to the optical density belongs to carbonates, and 5%, to hydroxides, while the contribution of the remaining classes is on the noise level. Among carbonates, 77% of the contribution is due to the spectrum of another sample of hydromagnesite (San Benito County, California, United States; sample no. 79228, Fersman Mineralogical Museum, Russian Academy of Sciences) included into the basis. The little (5%) involvement of hydroxides in the resolution may be explained by variation of band intensities of hydroxyl groups in hydromagnesite from one sample to another, for example, owing to isomorphic substitutions in the cation part.

A typical situation is when the spectrum of the examined mineral is absent in the basis, but there are spectra of mineral species pertaining to the same group or isomorphic series. For example, 12 nonzero components of the resolution were found for the spectrum of the beryllosilicate telyushenkoite, $CsNa_6Be_2(Si,Al,Zn)_{18}O_{39}F_2$ (Fig. 8b). Beryllosilicates contribute 84% of the optical density, with 7% being contributed by the framework aluminosilicate sodalite. Among the beryllosilicates, 91% of the optical density is due to leifite, $Na_6Be_2Si_{16} \cdot Al_2O_{39}(OH) \cdot 5H_2O$, which is similar to telyushenkoite in structure and chemical composition.

A similar result was obtained in analysis of a uranyl nesosilicate, sodium boltwoodite, $(H_3O)Na(UO_2)(SiO_4) \cdot H_2O$ (Fig. 8c). Of the 19 nonzero components of the resolution, 81% of the optical density is due to silicates, with 72% of the silicate contribution being from uranyl nesosilicates: boltwoodite, $HK(UO_2)(SiO_4) \cdot 1.5H_2O$, and uranophane, $Ca(UO_2)_2(SiO_3OH)_2 \cdot H_2O$.

A somewhat different situation occurs when vermiculite, pertaining to the phyllosilicate subclass, is analyzed (Fig. 8d). Because of the very wide bands characteristic of the IR spectrum of vermiculite, a high-quality approximation yields 36 nonzero components of the resolution. Along with silicates (78%), small nonzero contributions were made by nine other mineral classes. As expected, among silicates, phyllosilicates make the major contribution (68%), with another 10% being due to ring silicates, which probably indicates tetrahedral rings in the structure of vermiculite.

The results of examination of gordaite, $NaZn_4(SO_4)(OH)_6Cl \cdot H_2O$, are as follows: sulfate minerals, 58%; hydroxides, 9%; and contributions of other classes ≤7%, including chlorides, 5%. These contributions fit the chemical composition of the mineral with a good quality of spectrum approximation (Fig. 8e). At the same time (and this is typical of sulfates), silicates make an appreciable contribution to the resolution; for other sulfates, phosphates occasionally make a substantial though not the main contribution to the approximation. The contribution of alien classes decreases with increasing number of spectra in the basis.

Major problems in application of the functional method. In some cases, the application of the functional–geometric method does not yield the expected results. This may be seen in poor approximation of the analyzed spectrum or unsatisfactory recognition of a mineral as belonging to a specific class of chemical compounds or structural type. The examples given below illustrate typical problems and make it possible to understand their causes.

Figure 9a shows an analysis of the IR spectrum of the ammonium phosphate spheniscidite, $(NH_4^+)Fe_2^{3+}(PO_4)_2(OH) \cdot 2H_2O$, from iron ore of the Kerch basin. Sixteen spectra made nonzero contributions to the resolution, with a low quality of approximation. The mineral was identified as phosphate. The contribution of phosphates to the optical density is 50%, whereas other classes contributed no more than 11%. The relatively low contribution of phosphates and poor quality of fitting of the analyzed spectrum are explained by a lack of phosphates close in structure to spheniscidite (such as leucophosphite and tinsleyite), as well as ammonium phosphates, in the basis. The noticeable contribution of carbonates (8%) with spectra fitting the ammonium band with a maximum around 1420 cm^{-1} in the spectrum of spheniscidite is indicative.

A low quality of approximation in the functional–geometric analysis of the hanksite, $KNa_{22}(SO_4)_9(CO_3)_2Cl$, spectrum (Fig. 9b) did not hinder identification of this mineral. Only six spectra (less than 1% of the basis set), of which 83% (according to integral optical density) are due to sulfates and 17% to carbonates, made a nonzero contribution to the resolution. This result coincides almost exactly with the hanksite formula, where SO_4 groups amount to 82% of the oxygen-bearing anions and CO_3 groups make up the remaining 18%. In this example, good recognition with poor fitting is related to mutual compensation of positive and negative deviations of the spectrum recovered from the basis in the region of the strongest absorption of carbonate groups (1350–1550 cm^{-1}) relative to the analyzed curve.

The very poor approximation obtained as a result of functional–geometric analysis of the spectrum of the zirconium carbonate weloganite $Sr_3Na_2Zr(CO_3)_6 \cdot 3H_2O$ (Fig. 9c) is caused by the high force characteristics of zirconium (an element that is not typical of carbonates), which results in anomalously strong shifts and splitting of stretching and bending bands of carbon-

ate groups. Nevertheless, carbonates make the major contribution (74%) to the resolution of the weloganite spectrum; borates (16%) and organic compounds (10%) make an additional contribution to the approximation. Among carbonates, 47% of the integral optical density is due to andersonite and 45%, to donnayite (a Zr-free carbonate close in structure to weloganite).

In the case of metamict minerals, functional–geometric analysis, as a rule, does not lead to the fitting of the spectrum by a predominant class or subclass of minerals. The evident reason for this is the nature of metamict minerals, whose primary structure is broken down under the effect of radioactive irradiation. An analysis of the spectrum of metamict ekanite, $ThCa_2Si_8O_{20}$, illustrates this circumstance (Fig. 9d). The good fitting of the spectral curve, not surprising if the 48 nonzero components of the resolution are taken into account, is combined with a wide distribution of components by classes and subclasses corresponding to a multicomponent mixture of the following composition (in descending order of contribution): 23% framework silicates, 15% oxides, 13% ring silicates, 10% silicates of complex structure, 5% chain silicates, 4% phyllosilicates, etc.; noise contributions were made by silicates of other subclasses, phosphates, sulfates, chlorides, borates, and arsenates. It may be suggested that the distribution obtained reflects the real structure of amorphous metamict matter (more exactly, the set of local structures). The significant contribution of oxide components indicates a partial breakdown of primary silicate into a mixture of oxides accompanied (as inferred from the contribution of framework silicates) by condensation of Si-tetrahedrons. If this suggestion is valid, the functional–geometric method may be a convenient technique for studying real structures of amorphous hydrosilicate minerals (“allophanoids”) and silicate glasses and melts.

Completeness of the basis, ensuring geometric closeness of the analyzed spectrum to the cone of spectra of mixtures, is a necessary condition for successful application of the functional–geometric method. If no spectra of compounds related to the analyzed mineral are present in the basis, then the result of resolution of the projection remains uninformative even in the case of a good approximation. The analysis of the uranyl oxide studtite, $UO_4 \cdot 4H_2$, on a basis devoid of uranyl oxides is a striking example (Fig. 9e). In this case, the linear combination of spectra of arsenates (15%), polyborates (9%), orthoborates (7%), beryllosilicates (15%), carbonates (7%), iodides (10%), ring silicates (8%), sulfate-silicates (7%), and other compounds gives the best square approximation. Despite the good accuracy of such an approximation (the relative square deviation is 3%), it is formal and direct component-by-component decomposition of the projection does not yield a clear physical interpretation. It cannot be ruled out that the correct interpretation of the functional–geometric analysis results in this example requires a transition from the resolution of the spectrum projection by the initial basis to resolution by independent marginal directions of the cone.

As was mentioned above, the identification of a mineral with the functional–geometric method does not involve difficulties if the spectrum of this mineral is contained in the basis. In this case, the minimum variant of fast one-dimensional analysis with enumeration of the list of basis spectra and the variant of maximum analysis with the complete basis are equally applicable. In addition, in the overwhelming majority of cases, analogues (minerals pertaining to the same class or group) of a mineral having a crystal structure are identified quite reliably if they occur in the basis.

CONCLUSIONS

Thus, traditional discrete standard IR spectroscopy is an effective tool for minerals having a characteristic set of narrow bands. First of all, these are oxygen compounds with a high degree of cation ordering. The transition to examination of a continuous spectral curve using integral comparison functionals substantially widens the possibilities of analysis using reference samples because this method does not require narrow peaks. In particular, new possibilities are offered by the development of geometric analysis of spectral curves, in which an analyzed spectrum is compared with the cone of probable spectra of mixed substances incorporated into a database. This generalization does not presuppose the occurrence of the studied mineral in the list of mineral species included in the database, but provides for the best approximation of the spectrum of its absorption coefficient by a linear combination of known components with nonnegative coefficients. Practice shows that in most cases only a small part of the basis is involved in such a combination with nonzero coefficients. The spectra of minerals having the greatest crystallochemical cognation to the analyzed mineral possess the largest weights. The physical mechanism of this phenomenon is not completely clear.

The necessity of having an extensive database of IR spectra measured with a high accuracy (~1%) in the mid-IR range is a serious obstacle limiting the application of functional–geometric approaches.

ACKNOWLEDGMENTS

This study was supported by the Russian Foundation for Basic Research in cooperation with the Ministry of Industry and Science of Moscow oblast (project no. 04-01-97202-r2004naukograd).

REFERENCES

1. N. V. Chukanov and V. A. Dubovitsky, “New Aspects of Using of Infra-Red Spectroscopy in Mineralogical Studies,” in *Proceedings of Annual Session of Moscow Division Mineralogical Society, Moscow, November 4–5,*

2003 (IGEM RAS, Moscow, 2003), pp. 129–130 [in Russian].

2. N. V. Chukanov and St. Moeckel, "Atencioite, $Ca_2Fe^{2+}Mg_2Fe_2^{3+}Be_4(PO_4)_6(OH)_4 \cdot 6H_2O$, a New Mineral," in *Proceedings of the III Intern. Symp. on Mineral Diversity—Research and Preservation* (Sofia, 2005), p. 16.
3. N. V. Chukanov, V. A. Dubovitsky, and S. A. Vozchikova, "Expert System for Identification of Mineral Mixtures by IR Spectroscopy," in *Proceedings of Annual Session of Moscow Division of Mineralogical Society on Role of Mineralogical Studies in Solution of Environmental Problems, May 28–30, 2002* (VIMS, Moscow, 2002), pp. 187–189 [in Russian].
4. N. V. Chukanov and I. V. Pekov, "Heterosilicates with Tetrahedral-Octahedral Frameworks: Mineralogical and Crystal-Chemical Aspects," in *Reviews Mineral. Geochem., Vol. 57: Micro and Mesoporous Mineral Phases*, Ed. by G. Fettaris and S. Merlino (2005), pp. 105–143.
5. N. V. Chukanov, M. M. Moiseev, I. V. Pekov, et al., "Nabalamprofillite $Ba(Na,Ba)\{Na_3Ti[Ti_2O_2Si_4O_{14}](OH,F)_2\}$, New Layered Titanosilicate of Lamprofillie Group from Inagli and Kovdor Alkaline–Ultramafic Plutons, Russia," Zap. Vseross. Mineral. O–va **133** (1), 59–72 (2004).
6. N. V. Chukanov, M. M. Moiseev, R. K. Rastsvetaeva, et al., "Golyshevite $(Na,Sa)_{10}Ca_9(Fe^{3+},Fe^{2+})_2Zr_3NbSi_{25}O_{72}(CO_3)(OH)_3 \cdot H_2O$ and Mogovidite $N_9(Ca,Na)_6Ca_6(Fe^{3+},Fe^{2+})_2Zr_3S_{25}O_{72}(CO_3)(OH,H_2O)_4$, New Minerals of Eudialite Group from High-Ca Peralkaline Pegmatites of the Kovdor Pluton, Kola Peninsula," Zap. Vseross. Mineral. O–va **134** (6), 36–47 (2005).
7. N. V. Chukanov, I. V. Pekov, A. E. Zadov, et al., "Ikranite $(Na,H_3O)_{15}(Ca,Mn,REE)_6Fe_2^{3+}Zr_3(\square,Zr)(\square,Si)Si_{24}O_{66}(O,OH)_6Cl \cdot nH_2O$ and Raslakite $Na_{15}Ca_3Fe_3(Na,Zr)_3Zr_3(Si,Nb)(Si_{25}O_{73})(OH,H_2O_3(Cl,OH))$, New Minerals Species of Eudialite Group from Lovozero Pluton," (Zap. Vseross. Mineral. O–va **132** (5), 25–33 (2003a) [in Russian].
8. N. V. Chukanov, I. V. Pekov, R. K. Rastsvetaeva, et al., "Clinobarylite $BaBe_2Si_2O_7$, New Mineral from Khibiny Pluton, Kola Peninsula," Zap. Vseross. Mineral. O–va **132** (1), 29–37 (2003b).
9. N. V. Chukanov, R. K. Rastsvetaeva, St. Moeckel, et al., "New Mineral Atencioite $Ca_2Fe^{2+}\square Mg_2Fe_2^{2+}Be_4(PO_4)_6(OH)_4 \cdot 6H_2O$ and Its Relationships with Other Minerals of Rosherite Group," in *New Data on Minerals* (2006) (in press).
10. V. A. Dubovitsky and V. I. Irzhak, "Stable Determination of Relaxon Spectrum from the Data on Mechanical Relaxation of Polymers," Vysokomol. Soed., Series B **47** (1), 121–143 (2005).
11. V. A. Dubovitsky and I. A. Milyutina, *Histogram Method for Digital Analysis of Multicomponent Kinetics of DNK Reassociation* Preprint (Inst. Chem. Physics, Chernogolovka, 1985).
12. V. A. Dubovitsky, N. V. Chukanov, and S. A. Vozchikova, "Complex Identification of Inorganic Compounds from a Curve of IRR Absorption," Khim. Fiz. **23** (5), 90–100 (2004).
13. L. Fanfani, P. Zanazzi, and A. R. Zanzari, "The Crystal Structure of Triclinic Roscherite," Tschermaks Mineral. Petrogr. Mitt. **24**, 169–178 (1977).
14. A. V. Fiacco and G. P. McCormick, *Nonlinear Programming: Sequential Unconstrained Minimization Techniques* (Wiley, New York, 1968; Mir, Moscow, 1972).
15. C.L. Lawson and R. J. Hanson, *Solving Least Square Problems* (Prentoce-Hall, Englewood Cliffs, 1974; Nauka, Moscow, 1986).
16. *Modern Vibrational Spectroscopy of Inorganic Compounds*, Ed. by E. N. Yurchenko (Nauka, Novosibirsk, 1990) [in Russian].
17. I. V. Pekov, N. V. Chukanov, G. Ferraris, et al., "Shirokshinite, $K(NaMg_2)Si_4O_{10}F_2$, a New Mica with Octahedral Na from Khibiny Massif, Kola Peninsula: Descriptive Data and Structural Disorder," Eur. J. Mineral. **15**, 447–454 (2003).
18. I. V. Pekov, N. V. Chukanov, P. Tarasoff, et al., "Gjerdingenite-Na and Gjerdingenite-Ca: Two New Minerals of the Labuntsovite Group," Can. Mineral. **45**, 529–539 (2007).
19. R. W. Pohl, *Optik und Atomphysik* (Springer, Berlin, 1963; Mir, Moscow, 1966).
20. R. K. Rastsvetaeva, A. V. Barinova, N. V. Chukanov, and A. Petrashko, "Crystal Structure of High-Magnesium Triclinic Analogue of Greifensteinite," Dokl. Akad. Nauk **398** (4), 492–497 (2004).
21. G. A. Sidorenko, N. V. Chukanov, N. I. Chistyakova, et al., "Uramarsite $(NH_4,H_3O)_2(UO_2)_2(AsO_4,PO_4)_2 \cdot 6H_2O$, New Mineral of Metaotenite Group," Dokl. Akad. Nauk (in press).
22. *Vibrational Spectroscopy: Modern Trends,* Ed. by A. J. Barnes and W.J Orville-Thomas (Elsevier, Amsterdam, 1977; Mir, Moscow, 1981) [in Russian].
23. S. A. Vozchikova, V. A. Dubovitsky, and N. V. Chukanov, "Complex Identification of Chemical Compounds from Curve of IR Absorption," in *Proceedings of the XVII Symposium on Modern Chemical Physics* (Tuapse, 2005), pp. 152–153.